CSIRO PUBLISHING

www.publish.csiro.au/journals/ijwf *International Journal of Wildland Fire*, 2005, **14**, 249–254

Remote classification of head and backfire types from MODIS fire radiative power and smoke plume observations

Alistair M. S. Smith[A,C] *and Martin J. Wooster*[B]

[A]Department of Forest Resources, University of Idaho, Moscow, ID 83844-1133, USA.
[B]Department of Geography, King's College London, London, WC2R 2LS, UK. Telephone: +44 207 848 2577; fax: +44 207 848 2287; email: martin.wooster@kcl.ac.uk
[C]Corresponding author. Telephone: +1 208 885 1009; fax: +1 208 885 6226; email: alistair@uidaho.edu

Abstract. The classification of savanna fires into headfire and backfire types can in theory help in assessing pollutant emissions to the atmosphere via relative apportionment of the amounts of smouldering and flaming combustion occurring, and is also important when assessing a fire's ecological effects. This paper provides a preliminary assessment of whether a combination of visible and thermal satellite remote sensing can be used to classify fires into head and backfire categories. Remote determination of the fire radiative power, alongside assessments of the prevailing direction of the wind (through identification of the fire-related smoke plumes) and the fire front propagation (through its relation to the previously burned area) were used to infer the fire type category and to calculate 'radiative' fireline intensity (FLI). The ratio of radiative FLI for the head and backfire categories was found similar to that of *in situ* fireline intensity measurements, but the magnitudes of the radiative FLI values were around an order of magnitude lower. This agrees with other data suggesting that a fire's radiative energy is around an order of magnitude lower than the fuel's theoretical heat yield, and suggests that the remote measurement of radiative FLI and classification of headfire and backfire types is a realistic proposition for large wildfire activity.

Additional keywords: carbon; fire; global emission budgets; intensity; radiative energy.

Introduction

Assessment of wildfire chemical and aerosol emissions to the atmosphere is vital for global climate change and atmospheric chemistry research, in addition to being an important component of attempts to model local and regional air quality in many areas (Crutzen and Andreae 1990; Andreae and Merlet 2001; Hardy *et al*. 2001). In most environments, the emission of pyrogenic gases (carbon dioxide, nitrogen dioxide, etc.) represents a net source of compounds that can contribute to atmospheric chemistry reactions (Andreae and Merlet 2001). Wildfire emissions are particularly large for southern Africa savannas, which estimates suggest are responsible for between one-fifteenth and one-fifth of global biomass burning emissions (Andreae 1991; Scholes *et al*. 1996*a*). However, within the savanna biome, vegetation typically returns to a steady state of green biomass post-fire, and this regrowth is believed to sequester a similar amount of elements as that released during combustion (Hao *et al*. 1990; Andreae 1991; Houghton 1991). This arguably makes the pyrogenic aerosol emissions and their short-term effect on Earth's clouds, rainfall and radiation budget one of the most important atmospheric implications of savanna burning, though the release of other pollutant species such as CO also has important short-term air quality implications (Hardy *et al*. 2001).

Regional scale emission estimates for savanna fires are generally undertaken via model-based approaches that combine information on the amount of emitted gas species per unit mass of fuel burned, with estimates of the burned area, fuel load and the proportion of the available fuel actually combusted (Seiler and Crutzen 1980; Kasischke and Bruhwiler 2003). The large-scale, unpredictable and isolated nature of many wildfires has necessitated the use of remotely sensed data in the emissions estimation process. Indeed, imagery collected by Earth Observation (EO) satellites has been used to provide information of each of the latter model parameters, most commonly and reliably the area burned (e.g. Pereira 1999; Smith *et al*. 2002; Hudak and Brockett 2004), but also the available fuel load (via estimates of net primary productivity; Law and Waring 1994; Gower *et al*. 1999) and the combustion completeness (via measures relating to the fire severity; Landmann 2003; van Wagtendonk *et al*. 2004; Smith

 10.1071/WF05012 1049-8001/05/030249

et al. 2005*a*). Though these applications of EO data have undeniably assisted in greatly improving the quantification of pyrogenic emissions, there still exists the potential to further expand the use of remote sensing. In particular, French *et al*. (2004) note that improved, remotely derived information on fire severity is key to enhanced EO-derived parameterizations. Information on the type of fire is important in this context, since the fire severity and the particular chemical and aerosol constituents of the smoke can vary between different fire types, most notably between smouldering and flaming combustion (Andreae and Merlet 2001; Hardy *et al*. 2001; Kasischke and Bruhwiler 2003).

One source of information on fire that has been widely used during *in situ* and other studies is the classification of fire events into headfires and backfires, meaning fires that are moving predominately with or against the wind (Davis 1959; Trollope *et al*. 1996). The importance of this classification in part stems from the fact that headfires and backfires typically exhibit somewhat different combustion characteristics. Research in tropical savannas has demonstrated that headfires in general attain higher temperatures due to the increased prevalence of flaming combustion. This is in contrast to backfires, where a greater proportion of smouldering, lower temperature combustion is more common (Batchelder and Hirt 1966; Trollope 1984; Trollope *et al*. 1996). Importantly, the relative emission of different chemical compounds by a fire is strongly dependent on the relative incidence of flaming and smouldering combustion, and it is well known that, although between 20% and 90% of total pyrogenic emissions occur during the flaming stage, the relative emissions of partially combusted products such as smoke particulates, methane, and CO increase during the smouldering stage (Scholes *et al*. 1996*b*; Hardy *et al*. 2001).

Head and backfire categorization is also important with regard to the assessment of fire ecological effects, such as plant mortality. Such effects are in part dependent both on the intensity of the fire (i.e. how much heat is released per unit time) and by the fire residence time (Trollope *et al*. 1996). Though savanna backfires are typically characterized by lower fire intensities when compared to headfires (Table 1), they generally have longer residence times since the fire front is moving against the wind and thus typically has a far lower rate of spread (Shea *et al*. 1996). This characteristic can result in backfires exhibiting both an overall increased combustion completeness and a higher degree of plant mortality, due to the fire-affected areas retaining elevated temperatures (e.g. $>100^{\circ}$C) for longer (Batchelder and Hirt 1966; Trollope *et al*. 1996). EO-based classification of fires into headfire and backfire categories could therefore provide an additional source of data for emission procedures and for the assessment of fire ecological effects. Here we indicate an approach to infer this classification via the use of satellite imagery collected in the visible (0.5–0.7 μm) and middle infrared ($\sim$4 μm) spectral regions.

Table 1. Headfire and backfire fireline intensities (FLI) in southern African savannas, determined from *in situ* measurements via calculations involving fuel theoretical heat yield, fire rate of spread, and fuel mass combusted

	FLI (kW m^{-1})	Reference
Headfire	4048–10 906	Stocks *et al.* (1996)
	93–3644	Trollope *et al.* (1996)
	2810 ± 893	Trollope (1996)
	43–9476	Hely *et al.* (2003)
	130–9274	Smith (2004)
Backfire	20–160	Trollope *et al.* (1996)
	77 ± 29	Trollope (1996)

Fire radiative power and radiative fireline intensity

Thermal remote sensing in the middle infrared (MIR) spectral region can provide information on the rate of energy emission from fires, the so-called fire radiative power (FRP) (Kaufman *et al*. 1996, 1998; Wooster 2002; Wooster *et al*. 2003, 2004; Riggan *et al*. 2004). FRP can be derived from spectral measurements made by the Moderate Resolution Imaging Spectroradiometer (MODIS) onboard the EOS TERRA and AQUA satellites, and relates directly to the fire intensity and rate of fuel consumption (Kaufman *et al*. 1998; Wooster *et al*. 2003). The integration of FRP over the fire lifetime provides a measure of the fire radiative energy (FRE), which is proportional to the total fuel mass combusted (Kaufman *et al*. 1996; Wooster 2002). As an example of its use, FRP data from MODIS were recently used to indicate the tendency for boreal forest fires to burn less intensely in Russian forests than in North American forests (Wooster and Zhang 2004), a fact apparently related to the near-absence of Russian plant functional types that promote the growth of surface fires into the canopy via, for example, the retention of low-reaching dead branches that act as ladder fuels (Wirth 2005). Such ladder fuels are much more common in boreal North America, which as a result experiences a higher incidence of intense crown fires than do Russian boreal forests.

Here we use the FRP technique to measure the rate of thermally emitted energy from the classified head and backfires, and from a combination of FRP and fire-front length deduce a measure of 'radiative' fireline intensity (FLI). We compare the ratio of radiative FLI for headfires and backfires to the ratio of *in situ*-derived FLI for the same fire types reported in the literature.

Methods

The primary dataset used in this initial, small-scale study comprised selected MODIS level 1b radiance images from both the TERRA and AQUA satellites, providing both FRP retrievals and smoke plume identification. Data were obtained for fires in northern and central Botswana during the 2001 and 2004 dry seasons (August to November). A secondary dataset was the MODIS 'thermal anomaly' (MOD14) product derived from each level 1b image, since this product

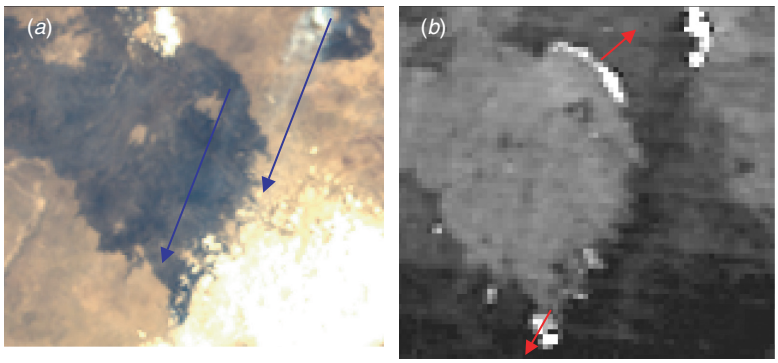

Fig. 1. Inferring the direction of the prevailing wind and fire front propagation from MODIS visible and middle infrared (MIR) channel imagery. (*a*) MODIS true colour composite (RGB) and (*b*) MIR channel 21 (3.9 μm) image of burned areas in central Botswana. In (*a*), arrows denote the general direction of the smoke plume, and therefore the wind whilst, in (*b*), arrows denote the direction of propagation of the two fire fronts away from the areas they have previously burned. The upper fire is moving in a direction almost directly against the wind, so is classified as a backfire, whilst the lower fire is moving in a direction more inclined with the wind, and so is classified as a headfire.

contains a mask corresponding to the location of all detected fire pixels (Justice *et al*. 2002). Data were collected from both satellite platforms and from multiple dates to assess reproducibility of the results under different dry season and diurnal conditions. Information of the typical available fuel load for the study area was obtained from the SPOT VEGETATION dry matter productivity product (acquired August 2001; http://free.vgt.vito.be/) and from *in situ* field surveys during October 2001 (Smith *et al.* 2005*b*).

Remotely inferring fire type

Following the broad definitions of Davis (1959) a fire was considered as a headfire if, at the time of image acquisition, the fire front was seen to be travelling in a direction more aligned with the prevailing wind. Similarly, a fire was considered as a backfire if the fire front was travelling more in a direction against the prevailing wind.

The MOD14 product fire mask was used to identify groups of contiguous active fire pixels present in the level 1b imagery, each cluster of active fire pixels being hereafter referred to as a single 'fire'. Only fires whose contributing fire pixels lay within 40° of nadir were used in order to limit the influence of the MODIS 'bow-tie' effect, which causes ground areas (including fires) imaged towards the edge of the swath to be recorded twice in successive scans (Wolfe *et al*. 2002). Fires needed to be three or more pixels in length to be considered for further analysis, in order that the approximate fire front length could be estimated and used in the calculation of radiative FLI. Using the MIR channel radiance data present in the MODIS level 1b imagery, the strong signature of the active fire pixels identified in the MOD14 fire product could clearly be seen, along with the related burned area, and the direction of travel of the fire front inferred from the relationship between these two (Fig. 1*b*). Using the MODIS visible channel radiance data, the direction of travel of the smoke plume associated with each fire could also be determined, and used to infer the predominant wind direction (Fig. 1*a*). Fires were considered for headfire/backfire categorization only if:

(1) Smoke plumes were clearly present at that fire or an adjacent fire; and
(2) Fire fronts were clearly travelling with or against the wind.

Fires in which no nearby smoke plumes were visible were excluded from the analysis, as were fires travelling perpendicular to the wind direction (i.e. flanking fires).

The methodology assumes that the rate of spread of the fire is much higher than the temporal variability of the wind direction (i.e. rapid changes in the wind direction do not result in misclassifications of the fire into headfire or backfire types). It further assumes that the direction of the smoke plume correctly indicates the prevailing wind direction at the surface, despite the complexity of the local fire-induced airflow and the potentially rapid changes of wind direction with height due to decreasing surface friction (i.e. Eckman spiral).

Derivation of FRP and radiative FLI

As noted previously, Kaufman *et al*. (1998) and Wooster *et al*. (2003) have demonstrated that the FRP of a pixel containing flaming combustion is about an order of magnitude greater than one containing a fire covering the same ground area but which is undergoing smouldering combustion. This difference results from the higher temperatures involved in flaming combustion and the fact that FRP varies with the fourth power of the temperature. In a similar way, during *in situ* measurement campaigns, the FLI of southern African savanna headfires has been observed to be considerably higher than in backfires conducted in the same environment (Table 1).

Following Wooster *et al*. (2003), Eqn (1) was used to calculate FRP (kW) for each confirmed fire pixel within the MODIS MIR (3.9 μm) channel observations:

$$FRP = A_{\text{samp}}[1.89 \times 10^{7}(L_{\text{MIR,f}} - L_{\text{MIR,bg}})] \times 10^{-3}, \quad (1)$$

where FRP is in kW, and $L_{\text{MIR,f}}$ and $L_{\text{MIR,bg}}$ denote the radiance recorded in the MODIS MIR channel ($\text{W m}^{-2}\,\text{sr}^{-1}\,\mu\text{m}^{-1}$) at the fire and background 'non-fire' pixels respectively. A_{samp} is the MODIS ground sample area at the relevant scan angle of the observation.

ΣFRP for each fire front was calculated via summation of the individual pixel FRP measures, and radiative FLI (kW m^{-1}) calculated by dividing ΣFRP by the fire front length (in metres), the latter being determined from the MIR imagery (Fig. 1*b*).

Results

Results are presented in Table 2. The ΣFRP and radiative FLI of the headfires were consistently above that of the backfires, and this difference was apparent over all MODIS image acquisitions and times, indicating an apparent insensitivity of the relationship to diurnal and seasonal variations. On average, ΣFRP of the headfires was 38.5 times greater than that of the backfires, while the radiative FLI was a factor of 9.3 times greater. The radiative FLI of the headfires and backfires is an order of magnitude lower than the typical field-based FLI measures, and this agrees very well with the finding of M. J. Wooster, G. Roberts and G. L. W. Perry (unpublished data) that the fire radiative energy emitted by combusting vegetation and measured by a nadir-pointing MIR imager is approximately an order of magnitude lower than the fuel's theoretical heat yield. Importantly, for both radiative FLI and field-measured FLI, the mean ratio of the FLI values determined from headfires and backfires is approximately the same.

The results confirm that the combination of visible and middle infrared imagery provided by MODIS can indeed be used to remotely infer fire type within large-scale wildfires. Measures of the dry matter productivity obtained across the fire-affected areas were of the order of $4000\,\text{kg ha}^{-1}$, similar to that observed during natural wildfires in the study area (Smith *et al.* 2005*b*). Dry matter productivity did not vary substantially between areas in which the headfires and backfires occurred, suggesting that the differences observed between these fire types were not simply due to variations in available fuel load, but rather the rate of spread as controlled by the wind speed and direction in relation to the fire's direction of propagation.

Discussion and conclusion

The classification of savanna burns as headfires or backfires is potentially important for the assessment of combustion completeness and estimating the relative emissions of different smoke aerosol and trace gas species such as CO and CO_2. A remote sensing approach allows this assessment to be made over a much wider area than purely *in situ* measurements allow. By employing the FRP method along with an assessment of the fire front length, we have demonstrated a simple method to derive a measure of fire front intensity (kW m^{-1}) from MODIS, akin to the standard fire line intensity measure estimated *in situ*. Such information can also be

Table 2. Data for headfires and backfires classified via satellite remote sensing from MODIS
FLI, fireline intensity; FRP, fire radiative power

Date	Time	Satellite platform	Fire type	ΣFRP (MW)	Radiative FLI (kW m^{-1})	Fire front length (km)
19 Aug. 2001	08:55	TERRA	Head	1800	140	12.9
			Head	349	74	4.7
			Head	1568	114	13.8
			Back	76	7	11.5
			Back	132	21	6.2
			Back	47	14	3.4
05 Oct. 2004	08:50	TERRA	Back	138	24	5.9
			Head	1061	147	7.2
			Head	642	90	7.2
	11:35	AQUA	Head	5280	156	33.9
07 Oct. 2004	08:40	TERRA	Head	1013	86	11.8
			Head	9113	328	27.8
			Back	50	17	2.9
	11:25	AQUA	Head	12 482	290	43.0
30 Oct. 2004	08:45	TERRA	Head	745	105	7.1
			Mean Head	3405	153	16.9
			Range Head	12 132	253	38.3
			Mean Back	88	17	6.0
			Range Back	91	17	3.4
			Head : Back mean ratio	38.5	9.3	2.8

of value in assessment of the fire ecological effects, and the acquisition of multiple MODIS images during the course of a fire could allow the production of a spatio-temporal map of radiative FLI and fire type across the area burned. The FRP approach can be used with imagery of any large-scale wildfire events where unsaturated MIR channel data are obtained. Imagery from higher spatial resolution MIR-equipped sensors such as the BIRD hotspot recognition sensor (Wooster *et al*. 2003; Zhukov *et al*. 2005) would allow a much more detailed assessment of fire front length, and also analysis of fires that were significantly smaller than those capable of being studied by MODIS. Further research is required to repeat the analysis for forest fires, where the added dimension of crown *v.* surface fires leads to additional, very notable FRP differences (Wooster and Zhang 2004). Direct comparisons between *in situ*-derived FLI and EO-derived radiative FLI are also warranted. Although the methodology presented in this preliminary study is labour intensive, an automated procedure could feasibly be developed to automatically calculate from MODIS or similar data the area previously burned, the propagation direction of the fire fronts with respect to the wind, and the measures of ΣFRP and radiative FLI.

Acknowledgements

Alistair Smith is part of the Forest Public Access Resource Center (ForestPARC) and is supported with funding from the Upper Midwest Aerospace Consortium (UMAC), which is in turn supported with funds from NASA. Methods developed here were in part supported by NERC grant NER/Z/S/2001/01027. MODIS data were acquired as part of NASA's Earth Science Enterprise with algorithms developed by the MODIS Science Teams. Data were archived and distributed by the Goddard DAAC.

References

Andreae MO (1991) Biomass burning: its history, use, and distribution and impact on environmental quality and global climate. In 'Global biomass burning: atmospheric, climatic and biospheric implications'. (Ed. JS Levine) pp. 3–21. (MIT Press: Cambridge, MA)

Andreae MO, Merlet P (2001) Emission of trace gases and aerosols from biomass burning. *Global Biochemical Cycles* **15**, 955–966. doi:10.1029/2000GB001382

Batchelder RB, Hirt HF (1966) Fire in tropical forests and grasslands. Technical Report: Contract No. DA19–129-AMC-229(N), United States Army. (United States Army Natick Laboratories: Natick, MA)

Crutzen PJ, Andreae MO (1990) Biomass burning in the tropics: impact on atmospheric chemistry and biogeochemical cycles. *Science* **250**, 1669–1678.

Davis KP (1959) Application of prescribed burning. In 'Forest fire: control and use'. (Eds AA Brown, KP Davis) pp. 507–537. (McGraw-Hill: New York)

French N, Goovaerts P, Kasischke ES (2004) Uncertainty in estimating carbon emissions from boreal forest fires. *Journal of Geophysical Research* **109**, D14S08. doi:10.1029/2003JD003635

Gower ST, Kucharik CJ, Norman JM (1999) Direct and indirect estimation of leaf area index, f_{APAR}, and net primary production of terrestrial ecosystems. *Remote Sensing of Environment* **70**, 29–51. doi:10.1016/S0034-4257(99)00056-5

Hao WM, Lui M-H, Crutzen PJ (1990) Estimates of annual and regional releases of CO_2 and other trace gases to the atmosphere from fires in the tropics, based on the FAO statistics for the period 1975–1980. In 'Fire in the tropical biota: ecosystem processes and global challenges'. (Ed. JG Goldammer) pp. 440–462. (Spinger-Verlag: New York)

Hardy CC, Ottmar RD, Peterson JL, Core JE, Seamon P (2001) 'Smoke management guide for prescribed and wildland fire 2001 edition.' National Wildfire Coordination Group, PMS 420–2.

Hely C, Alleaume S, Swap RJ, Shugart HH, Justice CO (2003) SAFARI-2000 characterisation of fuels, fire behaviour, combustion completeness and emissions from experimental burns in infertile grass savannas in western Zambia. *Journal of Arid Environments* **54**, 381–394. doi:10.1006/JARE.2002.1097

Houghton RA (1991) Biomass burning from the perspective of the global carbon cycle. In 'Global biomass burning: atmospheric, climatic and biospheric implications'. (Ed. JS Levine) pp. 321–325. (MIT Press: Cambridge, MA)

Hudak AT, Brockett BH (2004) Mapping fire scars in a southern African savannah using Landsat imagery. *International Journal of Remote Sensing* **25**, 3231–3243. doi:10.1080/01431160310001632666

Justice CO, Giglio L, Korontzi S, Owens J, Morisette JT, Roy D, Descloitres J, Alleaume S, Petitcolin F, Kaufman Y (2002) The MODIS fire products. *Remote Sensing of Environment* **83**, 244–262. doi:10.1016/S0034-4257(02)00076-7

Kasischke ES, Bruhwiler LP (2003) Emissions of carbon dioxide, carbon monoxide, and methane from boreal forest fires in 1998. *Journal of Geophysical Research* **108**, 8146.

Kaufman YJ, Remer LA, Ottmar RD, Ward DR, Li RR, Kleidman R, Fraser RS, Flynn L, McDougal D, Shelton G (1996) Relationship between remotely sensed fire intensity and rate of emission of smoke: SCAR-C experiment. In 'Biomass burning and global change'. (Ed. JS Levine) pp. 685–696. (MIT Press: Cambridge, MA)

Kaufman YJ, Kleidman RG, King MD (1998) SCAR-B fires in the tropics: properties and remote sensing from EOS-MODIS. *Journal of Geophysical Research* **103**, 31 955–31 968. doi:10.1029/98JD02460

Landmann T (2003) Characterizing sub-pixel Landsat ETM+ fire severity on experimental fires in the Kruger National Park, South Africa. *South African Journal of Science* **99**, 357–360.

Law BE, Waring RH (1994) Combining remote sensing and climatic data to estimate net primary production across Oregon. *Ecological Applications* **4**, 717–728.

Pereira JMC (1999) A comparative evaluation of NOAA/AVHRR vegetation indexes for burned surface detection and mapping. *IEEE Transactions on Geoscience and Remote Sensing* **37**, 217–226. doi:10.1109/36.739156

Riggan PJ, Tissell RG, Lockwood RN, Brass JA, Pereira JAR, Miranda HS, Miranda AC, Campos T, Higgins R (2004) Remote measurement of energy and carbon flux from wildfires in Brazil. *Ecological Applications* **14**, 855–872.

Scholes RJ, Kendall J, Justice CO (1996*a*) The quantity of biomass burned in southern Africa. *Journal of Geophysical Research* **101**, 23667–23676. doi:10.1029/96JD01623

Scholes RJ, Ward DE, Justice CO (1996*b*) Emissions of trace gases and aerosol particles due to vegetation burning in southern hemisphere Africa. *Journal of Geophysical Research* **101**, 23 677–23 682. doi:10.1029/95JD02049

Seiler W, Crutzen PJ (1980) Estimates of gross and net fluxes of carbon between the biosphere and the atmosphere from biomass burning. *Climatic Change* **2**, 207–247. doi:10.1007/BF00137988

Shea RW, Shea BW, Kauffman JB, Ward DE, Haskins CI, Scholes MC (1996) Fuel biomass and combustion factors associated with fires

in savanna ecosystems of South Africa and Zambia. *Journal of Geophysical Research* **101**, 23 551–23 568. doi:10.1029/95JD02047

Smith AMS (2004) Determining nitrogen volatilised in southern African savanna fires via ground based remote sensing. PhD Thesis, University of London.

Smith AMS, Wooster MJ, Powell AK, Usher D (2002) Texture based feature extraction: application to burn scar detection in Earth Observation satellite imagery. *International Journal of Remote Sensing* **23**, 1733–1739. doi:10.1080/01431160110106104

Smith AMS, Wooster MJ, Drake NA, Dipotso FM, Falkowski MJ, Hudak AT (2005*a*) Testing the potential of multi-spectral remote sensing for retrospectively estimating fire severity in African savanna environments. *Remote Sensing of Environment* in press.

Smith AMS, Wooster MJ, Drake NA, Perry GLW, Dipotso FM (2005*b*) Fire in African savanna: testing the impact of incomplete combustion on pyrogenic emissions estimates. *Ecological Applications* **15**, 1074–1082.

Stocks BJ, van Wilgen BW, Trollope WSW, McRae DJ, Mason JA, Weirich F, Potgeiter ALF (1996) Fuels and fire behavior dynamics on large-scale savanna fires in Kruger National Park, South Africa. *Journal of Geophysical Research* **101**, 23541–23550. doi:10.1029/95JD01734

Trollope WSW (1984) Fire in savanna. In 'Ecological effects of fire in South African ecosystems'. (Eds P de V Booysen, NM Tainton) Ecological Studies 48, Chapter 7, pp. 151–175. (Springer-Verlag: New York)

Trollope WSW (1996) Biomass burning in the savannas of Southern Africa with particular reference to the Kruger National Park in South Africa. In 'Biomass burning and global change'. (Ed. JS Levine) pp. 260–269. (MIT Press: Cambridge, MA)

Trollope WSW, Trollope LA, Potgieter ALF, Zambatis N (1996) SAFARI-92 characterization of biomass and fire behavior in the small experimental burns in Kruger National Park. *Journal of Geophysical Research* **101**, 23 531–23 540. doi:10.1029/96JD00691

van Wagtendonk JW, Root RR, Key CH (2004) Comparison of AVIRIS and Landsat ETM+ detection capabilities for burn severity. *Remote Sensing of Environment* **92**, 397–408. doi:10.1016/J.RSE.2003.12.015

Wirth (2005) Fire regime and tree diversity in boreal forests: implications for the carbon cycle. In 'Forest diversity and function. Ecological studies 176'. (Eds M Scherer-Lorenzen, Ch Körner, E-D Schulze) pp. 309–336. (Springer: Heidelberg)

Wolfe RE, Nishihama M, Fleig AJ, Kuyper JA, Roy DP, Storey JC, Patt FS (2002) Achieving sub-pixel geolocation accuracy in support of MODIS land science. *Remote Sensing of Environment* **83**, 31–49. doi:10.1016/S0034-4257(02)00085-8

Wooster MJ (2002) Small-scale experimental testing of fire radiative energy for quantifying mass combusted in natural vegetation fires. *Geophysical Research Letters* **29**, 2027. doi:10.1029/2002GL015487

Wooster MJ, Zhang YH (2004) Boreal forest fires burn less intensely in Russia than in North America. *Geophysical Research Letters* **31**, L20505. doi:10.1029/2004GL020805

Wooster MJ, Zhukov B, Oertel D (2003) Fire radiative energy for quantitative study of biomass burning: derivation from the BIRD experimental satellite and comparison to MODIS fire products. *Remote Sensing of Environment* **86**, 83–107. doi:10.1016/S0034-4257(03)00070-1

Wooster MJ, Perry GLW, Zhukov B, Oertel D (2004) Estimation of energy emissions, fireline intensity and biomass consumption in wildland fires: a potential approach using remotely sensed fire radiative energy. In 'Spatial modelling of the terrestrial environment'. (Eds R Kelly, N Drake, S Barr) pp. 177–199. (John Wiley & Sons: New York)

Zhukov B, Briess K, Lorenz E, Oertel D, Skrbek W (2005) Detection and analysis of high-temperature events in the BIRD mission. *Acta Astronautica* **56**, 65–71. doi:10.1016/J.ACTAASTRO.2004.09.014